ChemComm

Accepted Manuscript

This article can be cited before page numbers have been issued, to do this please use: X. Jiang, Z. Wang , H. Wang, Y. Zhuo, R. Yuan and Y. Chai, *Chem. Commun.*, 2017, DOI: 10.1039/C7CC05495E.

ROYAL SOCIETY OF CHEMISTRY

rsc.li/chemcomm

Dynamic Article Links ►
View Article Online
DOI: 10.1039/C7CC05495E

Cite this: DOI: 10.1039/c0xx00000x

www.rsc.org/xxxxxx

ARTICLE TYPE

A novel metal-organic framework loaded abundant *N*-(aminobutyl)-*N*-(ethylisoluminol) as high-efficiency electrochemiluminescence indicator for sensitive detection of mucin1 on cancer cells

Xinya Jiang, Zili Wang, Haijun Wang, Ying Zhuo, Ruo Yuan* and Yaqin Chai *

Received (in XXX, XXX) Xth XXXXXXXXX 20XX, Accepted Xth XXXXXXXXX 20XX
DOI: 10.1039/b000000x

Herein, a high-efficiency electrochemiluminescence (ECL) indicator of abundant *N*-(aminobutyl)-*N*-(ethylisoluminol) functionalized metal-organic framework (ABEI@Fe-MIL-101) was synthesized to construct biosensor for ultrasensitive assay of mucin1 on MCF-7 cancer cells with a coreactant H_2O_2-free strategy.

Cancer presents a major challenge to healthcare in the whole global.[1,2] To cure cancer, the necessary prerequisite is to identify the subtypes of cancer. Fortunately, cancer biomarkers (including proteins, carbohydrates, and mucleic acids) can be quantitatively detected, providing a great promise for the early diagnosis of cancer.[3] Nevertheless, the low abundance of biomarkers at the early stages of cancer and the heterogeneity among patients make a great challenge for early cancer detection. Therefore, it is very meaningful to construct a highly sensitive biosensor with simple and affordable technologies to detect trace protein on cancer cells. Among the analytical techniques, electrochemiluminescence (ECL) technology,[4] which is competitive with other technologies (electrochemical, fluorescence, colorimetric) due to its low background intensity, simple operation and high detection sensitivity, has been widely applied in bioanalysis.[5,6] As the classic ECL luminescence reagents, luminol or its derivative based ECL sandwich-type immunoassay have been applied to detect protein on cancer cells in recent.[7,8] In order to obtain a high ECL intensity, H_2O_2 was indispensable during the detecting process. Nevertheless, H_2O_2 was unstable and even harmful to cell or protein. Therefore, the development of new strategies to improve the ECL intensity of luminol or its derivative for biomarkers on cancer cell without the use of H_2O_2 is necessary, which will provide a biosafe environment for protein and cellular analysis.

With the aim of improving the sensitivity of immunoassay, many signal amplification strategies are involved in the construction of ECL biosensors.[9-12] Among these signal amplification strategies, immobilizing luminophore efficiently plays a key role in enhancing ECL intensity of biosensors since it directly determines the reaction quantity of luminophore, and then affects the luminous intensity of biosensors. In the early stage, Cui's group realized the immobilization of luminol or its derivatives via using them as reducing regent to synthesize luminol or its derivatives functionalized metal nanoparticles (MNPs).[13-15] However, luminol or its derivatives were only coexistence on the surface of MNPs through weak covalent interaction between MNPs and nitrogen atoms, which limited the immobilization amount of luminol or its derivatives to a certain extent. Recently, our group developed a novel method for *N*-(aminobutyl)-*N*-(ethylisoluminol) (ABEI) fixation *via* intercalating Dox-ABEI complex into tetrahedron DNA dendrimers.[16] This method increased the loading amount of ABEI effectively for ABEI could be embedded inside the tetrahedron DNA structure. However, considering that the tetrahedron DNA dendrimers may hinder the electron transfer, it is meaningful to develop a new and effective strategy for immobilizing luminol or its derivatives abundantly and efficiently.

Metal-organic frameworks (MOFs), which make up of metals and organic bridging ligands, have demonstrated superior physical and chemical properties.[17-19] Particularly, the tunable pore sizes, open cavities, and high surface areas of MOFs make them become an ideal candidate for storage,[20,21] catalysis,[22,23] biosensors[24,25] and so on. In recent, luminescent functional MOFs have become a promising optical sensing material.[26,27] Among the synthetic methods for luminescent functional MOFs, postsynthetic modification and encapsulation method were usually applied.[28-30] While postsynthetic modification method needed complex synthesis process, and encapsulation methods limited the load capacity for luminophore only existed in the inside of MOFs. Recently, to overcome these shortcomings, our group directly used luminophore $[Ru(dcbpy)_3]^{2+}$ as a ligand to synthesize MOFs with a good ECL performance for NT-proBNP detection.[31] However, the loading number of $[Ru(dcbpy)_3]^{2+}$ was still limited to a certain extent due to its large steric hindrance. Therefore, for the purpose of further increasing the loading number of luminophore, small molecule luminophore ABEI crosslinked 2-aminoterephhalic acid (NH_2-BDC) was utilized as a ligand to prepare ABEI functionalized MOFs in this study. Thanks to the high load capacity of ABEI in MOFs and the merits of MOFs, the obtained ABEI functionalized MOFs exhibited superior ECL property. Thus, ABEI functionalized MOFs would be a promising material in bioanalysis due to its superior ECL property, non-toxic and biocompatible.

In this work, a simple and ultrasensitive ECL biosensor based on a high-efficiency ECL indicator of novel MOFs immobilized with abundant ABEI (ABEI@Fe-MIL-101) was

View Article Online
DOI: 10.1039/C7CC05495E

fabricated to detect mucin1 (MUC1) on MCF-7 cancer cells with a H_2O_2-free strategy (Scheme 1). A significantly enhanced ECL intensity of the biosensor could be achieved since luminophore ABEI crosslinked NH_2-BDC was applied as the organic bridging ligand to synthesize Fe-MIL-101, resulting in large amounts of ABEI loaded in the skeleton structure of Fe-MIL-101. Furthermore, the ECL signal was further enhanced by controlling potential to convert dissolved oxygen into superoxide radicals ($O2^{\cdot-}$), which acted as the important intermediate in the ABEI ECL reaction. This method avoided the use of conventional co-reagent H_2O_2 to simplify the detection process and provide a biosafe environment for protein and cell assay. Satisfactorily, the constructed biosensor exhibited a low detection limit of 12 cells for MUC1 on MCF-7 cancer cells. This indicated that ABEI@Fe-MIL-101 with superior ECL property combined with H_2O_2-free detection mode may provide an effective strategy for ultrasensitive detection of biomarkers in the early diagnosis of cancer.

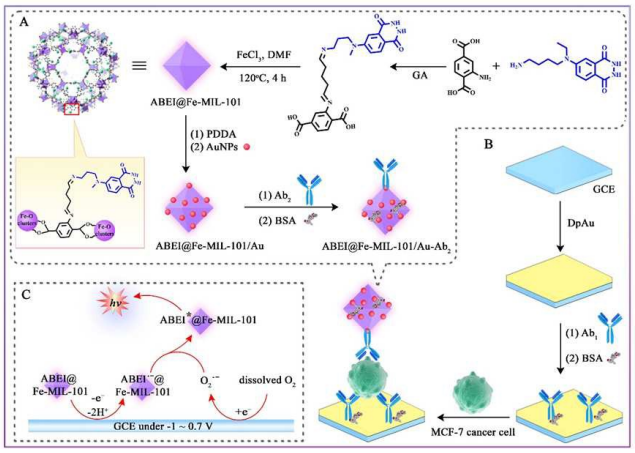

Scheme 1 The Schematic illustration of (A) the preparation of ABEI@Fe-MIL-101/Au-Ab_2 signal probe, (B) the fabrication of biosensor, and (C) the ECL reaction mechanism.

Scanning electron microscope (SEM) was first utilized to characterize the size and morphology of the proposed ABEI@Fe-MIL-101 nanomaterial. Figure 1A and B showed the SEM images of ABEI@Fe-MIL-101 nanomaterial at different dimensions. The SEM images exhibited that the ABEI@Fe-MIL-101 nanomaterial displayed an octahedron morphology and had a diameter of 50 ~ 200 nm. To further demonstrate the successful synthesis of the proposed ABEI@Fe-MIL-101 nanomaterial, X-ray diffraction (XRD) was used to characterize the structure of ABEI@Fe-MIL-101. Figure 1C showed the XRD pattern of the proposed ABEI@Fe-MIL-101 nanomaterial. It displayed that the typical lattice planes of Fe-MIL-101 could be observed in the obtained XRD pattern of ABEI@Fe-MIL-101.[32] These characterization results demonstrated that the luminescent-functionalized MOFs of ABEI@Fe-MIL-101 nanomaterial were synthesized successfully.

In addition, to prove the successful preparation of the proposed ABEI@Fe-MIL-101/Au nanocomposite, X-ray photoelectron spectroscopy (XPS) was used to investigate the elemental component. Figure S1A displayed the wide scan survey spectra of ABEI@Fe-MIL-101/Au, the characteristic peaks of Fe 2p, N 1s, C 1s, O 1s and Au 4f were clearly evident in the Figure. The existing Fe 2p, N 1s, C 1s, O 1s demonstrated the successful synthesis of ABEI@Fe-MIL-101. Furthermore, the Au 4f located at 83.08 eV indicated that the AuNPs effectively attached on the surface of ABEI@Fe-MIL-101. The amplified spectra of Fe 2p, N 1s, and Au 4f were revealed clearly in Figure S1B, C and D, respectively.

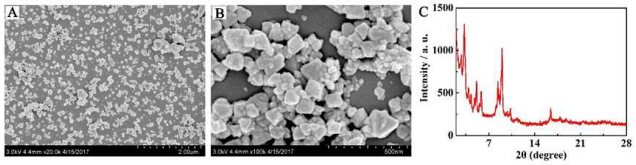

Figure 1. (A) and (B) were the SEM images of ABEI@Fe-MIL-101 at different dimensions. (C) XRD pattern of the proposed ABEI@Fe-MIL-101 nanomaterial.

To characterize the optical properties of the synthesized ABEI@Fe-MIL-101 nanomaterial, fluorescent (FL) spectrum, UV-vis absorption spectrum, and ECL spectrum were performed. Figure S2A, B exhibited the FL spectrum of ABEI@Fe-MIL-101 and pure ABEI, respectively. Compared with pure ABEI, the maximum excited wavelength of ABEI@Fe-MIL-101 changed to 348 nm from 378 nm, while the maximum emission wavelength of ABEI@Fe-MIL-101 was at 442 nm with a little redshift. Intuitively, the pure ABEI solution was colorless under ambient daylight (inset of Figure S2B), while the as-synthesized ABEI@Fe-MIL-101 solution displayed a brown color (inset in Figure S2A). However, under the 365 nm UV lamp radiation, two similar blue lights were both observed from the ABEI@Fe-MIL-101 (inset in Figure S2A) and pure ABEI (inset of Figure S2B). The results demonstrated that the luminophore ABEI was successfully loaded in the structure of Fe-MIL-101. To further confirm this, the UV-vis absorption spectra of the as-synthesized ABEI@Fe-MIL-101 nanomaterial was explored. As depicted in Figure S2C, compared with pure ABEI, the characteristic absorption peak of ABEI could be observed in ABEI@Fe-MIL-101 nanomaterial with a little redshift. In addition, the ECL emission spectra of ABEI@Fe-MIL-101 was also investigated by a series of optical filters, as shown in Figure S2D. The proposed ABEI@Fe-MIL-101 exhibited a distinct ECL peak at about 470 nm (blue curve) which was almost the same to the pure ABEI (red curve). Overall, the results indicated that the proposed ABEI@Fe-MIL-101 nanomaterial had the optical performances of ABEI and thus it could be applied in ECL analysis.

To investigate the possible ECL mechanism of ABEI under the potential of -1 ~ 0.7 V without H_2O_2, the ECL and its corresponding CV curves were measured. First, the ECL and CV curves of ABEI@Fe-MIL-101 nanomaterial under 0 ~ 0.7 V were tested. As displayed in Figure 2A, a low ECL emission was obtained from the ABEI@Fe-MIL-101 nanomaterial under the potential of 0 ~ 0.7 V (curve a1). In addition, a small oxidation peak was observed in its corresponding CV curve (curve b1) which was attributed to the oxidation of ABEI. However, under the potential of -1 ~ 0.7 V (Figure 2B), a strong ECL signal (curve a2) was observed from ABEI@Fe-MIL-101, which was about 20 times higher than that obtained from the potential of 0 ~ 0.7 V. The reason may be that dissolved O_2 was first reduced to OOH^- at around -0.58 V (curve b2) through the reduction reaction of dissolved $O_2 + H_2O + 2e^- \rightarrow OOH^- + OH^-$.[33] Then

View Article Online
DOI: 10.1039/C7CC05495E

the obtained OOH^- further became to $O_2^{\cdot-}$ through the reaction of $OOH^- - e^- \rightarrow HO_2^{\cdot} \rightarrow O_2^{\cdot-}$ under the positive potential. Thus, a significantly enhanced ECL signal could be obtained (Figure 2, curve a2) for the reason that the generated $O_2^{\cdot-}$ could react with oxidized ABEI to generate more excited state of ABEI.

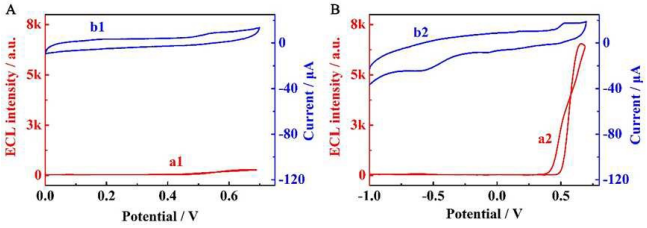

Figure 2. ECL and its corresponding CV curves of ABEI@Fe-MIL-101 under different scan potentials: (A) 0 ~ 0.7 V, (B) -1 ~ 0.7 V.

In order to obtain a high-efficiency luminous substance, three kinds of ABEI@Fe-MIL-101 nanomaterials were prepared via different synthetic approaches and then their ECL properties were investigated. As shown in Figure S3, the ABEI@Fe-MIL-101 obtained from directly doping ABEI in Fe-MIL-101 during the formation of Fe-MIL-101 exhibited a low ECL intensity about 766 a.u. (curve a). In addition, the ABEI@Fe-MIL-101 obtained from postsynthetic modification ABEI on Fe-MIL-101 through covalent cross-linking showed a slightly enhanced ECL intensity of about 1004 a.u. (curve b). Compared with these two ABEI@Fe-MIL-101 nanomaterials, the proposed ABEI@Fe-MIL-101 with use of ABEI crosslinked NH_2-BDC as organic bridging ligand in the formation of Fe-MIL-101 displayed a much higher ECL intensity about 6509 a.u. (curve c). The result indicated that using ABEI crosslinked NH_2-BDC as the organic bridging ligand to synthesize Fe-MIL-101 could lead to large amounts of ABEI loaded in the skeleton structure of Fe-MIL-101, providing a highly efficient method for ABEI immobilization.

To evaluate the quantitative range and sensitivity of the proposed ECL biosensor for MUC1, the biosensor was characterized by quantifying different concentrations of standard target MUC1 with ABEI@Fe-MIL-101/AuNPs-Ab_2 as signal probe. Figure 3A displayed the ECL profiles of various concentrations of MUC1 in the range of 1 fg mL^{-1} to 1 ng mL^{-1}. It obviously found that the ECL intensity of biosensor was proportional to the logarithm of MUC1 concentration (Figure 3B) with a linear regression equation of I_{ECL} = 1677.1 lg c + 11457 and a regression coefficient of 0.9977. Furthermore, the limit of detection was estimated to be 0.26 fg mL^{-1} according to $3S_B/m$ (S_B stands for standard deviation of bland, m stands for the slope of the obtained linear regression equation), which was more sensitive than most of the previously reported biosensors (Table S1).

To further evaluate the applicability of the proposed ECL biosensor, the biosensor was challenged to determinate MUC1 on MCF-7 cancer cells. As shown in Figure 3C, ECL intensities of different MCF-7 cancer cell numbers (20, 50, 100, 150, 200, and 250) were recorded in 2 mL PBS without H_2O_2. An obvious ECL intensity was observed from 20 MCF-7 cancer cells. In addition, a linear relationship between the ECL intensity and the number of MCF-7 cancer cells was obtained in this range, as depicted in Figure 3D. The regression equation was I_{ECL} = 36.8 N + 961.88 (N stands for the number of cancer cells) with a regression coefficient of 0.9971. The detection limit was down to 12 cells according to $3S_B/m$. Compared with other previous biosensors (Table S1), the proposed ECL biosensor based on the novel high-efficiency ECL indicator of ABEI@Fe-MIL-101 nanomaterials achieved a lower detection limit for MCF-7 cancer cells.

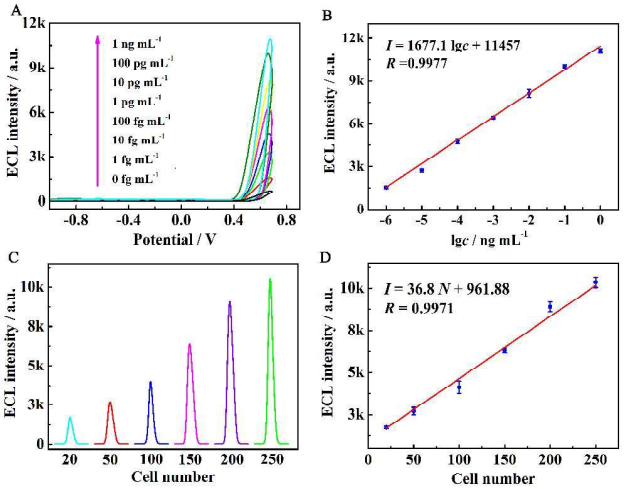

Figure 3. (A) The ECL curves obtained from different concentrations of MUC1 antigen. (B) The correlation of ECL intensity and the logarithm of MUC1 concentration. (C) The ECL curves obtained from different numbers of MCF-7 cancer cells. (D) The corresponding relationship between the ECL intensity and the number of MCF-7 cancer cells.

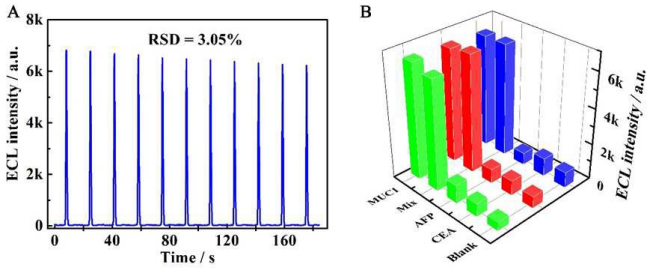

Figure 4. (A) Stability of the proposed ECL biosensor under continuous scanning for 11 cycles under 1 pg mL^{-1} MUC1 target. (B) Selectivity of the developed biosensor for MUC1 determination over other interference antigens.

As the important performances of a biosensor, the stability, selectivity, and reproducibility of the constructed ECL biosensor were investigated meticulously. Figure 4A depicted the ECL intensity upon continuous scanning for 11 cycles with 1 pg mL^{-1} MUC1 target. A relatively stable ECL intensity was obtained with a relative standard deviations (RSD) of 3.05%, indicating a satisfactory stability of the proposed biosensor. Figure 4B showed the ECL intensity toward to different targets, such as CEA, AFP, MUC1 and their mixture solution. As expected, a negligible ECL intensity was observed from interference antigen CEA or AFP incubated biosensor even they have a higher concentration (1ng mL^{-1}). While the target MUC1 (1pg mL^{-1}) and mixture solution containing MUC1 (1pg mL^{-1}) exhibited a significant ECL intensity even its concentration was 100-fold lower than interference antigen CEA or AFP. This result implied that the constructed ECL biosensor had the ability to discriminate the target from complex interference substances, indicating a

View Article Online
DOI: 10.1039/C7CC05495E

superior selectivity of this biosensor. In addition, a RSD for the reproducibility of this ECL biosensor was assessed to be less than 5% corresponding to five duplicate measurements for 1 pg mL^{-1} MUC1, suggesting an acceptable reproducibility of this developed immunosensor.

In conclusion, a simple and ultrasensitive ECL biosensor based on a high-efficiency ECL indicator of ABEI@Fe-MIL-101 nanomaterial was fabricated to detect mucin1 (MUC1) on MCF-7 cancer cells with a H_2O_2-free strategy. In order to enhance the sensitivity of ECL biosensor, the ABEI@Fe-MIL-101 nanomaterial was synthesized by using ABEI crosslinked NH_2-BDC as organic bridging ligand, resulting in abundant ABEI immobilized in the proposed ABEI@Fe-MIL-101 nanomaterial with high ECL luminous efficiency. In addition, the ECL intensity of the proposed ABEI@Fe-MIL-101 nanomaterial could be further enhanced due to the merits of the tunable pore sizes, open cavities, and high surface areas of MOFs. Furthermore, a H_2O_2-free strategy was achieved under the potential scan from -1.0 to 0.7 V, which not only simplified the detection process, but also expanded the ECL application in various fields, especially providing a more biosafe environment for cell detection. Thanks to the high-efficiency ABEI@Fe-MIL-101 ECL indicator and H_2O_2-free strategy, the proposed method may provide a simple, biosafe and sensitive detection for biomarkers on cancer cells in clinical diagnosis.

This work was financially supported by the NNSF of China (51473136, 21675129, 21575116), Chongqing graduate scientific research innovation project (CYB17061), and the China Postdoctoral Science Foundation (2016M602626), China.

Notes and references

Key Laboratory of Luminescence and Real-Time Analytical Chemistry, Ministry of Education, College of Chemistry and Chemical Engineering, Southwest University, Chongqing 400715, China. Tel: +86-23-68252277; Fax: +86-23-68253172. E-mail address: yuanruo@swu.edu.cn (R. Yuan), yqchai@swu.edu.cn (Y. Q. Chai).

† Electronic Supplementary Information (ESI) available: [experimental section; feasibility characterization of the ECL biosensor]. See DOI:10.1039/b000000x/

1 A. Jemal, F. Bray, M. M. Center, J. Ferlay, E. Ward and D. Forman, *Ca-Cancer J. Clin.* 2011, **61**, 69-90.

2 J. Ferlay, H. R. Shin, F. Bray, D. Forman, C. Mathers and D. M. Parkin, *Int. J. Cancer*, 2010, **127**, 2893-2917.

3 A. B. Chinen, C. M. Guan, J. R. Ferrer, S. N. Barnaby, T. J. Merkel and C. A. Mirkin, *Chem. Rev.* 2015, **115**, 10530-10574.

4 M. M. Richter, *Chem. Rev.* 2004, **104**, 3003-3036.

5 Y. Chen, S. W. Zhou, L. L. Li and J. J. Zhu, *Nano Today*, 2017, **12**, 98-115.

6 L. L. Li, Y. Chen and J. J. Zhu, *Anal. Chem.* 2017, **89**, 358-371.

7 F. F. Han, H. Jiang, D. J. Fang and D. C. Jiang, *Anal. Chem.* 2014, **86**, 6896-6902.

8 H. W. Shi, W. Zhao, Z. Liu, X. C. Liu, J. J. Xu and H. Y. Chen, *Anal. Chem.* 2016, **88**, 8795-8801.

9 X. Zhang, B. Zhang, W. J. Miao and G. Z. Zou, *Anal. Chem.* 2016, **88**, 5482-5488.

10 H. J. Wang, Y. L. Yuan, Y. Zhuo, Y. Q. Chai and Yuan, R. *Anal. Chem.* 2016, **88**, 2258-2265.

11 D. F. Wang, Y. Y. Li, Z. Y. Lin, B. Qiu and L. H. Guo, *Anal. Chem.* 2015, **87**, 5966-5972.

12 Y. Zhang, L. X. Wang, F. Luo, B. Qiu, L. H. Guo, Z. Q. Weng, Z. Y. Lin and G. N. Chen, *Chem. Commun.* 2017, **53**, 2910-2913.

13 G. X. Li, X. X. Yu, D. Q. Liu, X. Y. Liu, F. Li and H. Cui, *Anal. Chem.* 2015, **87**, 10976-10981.

14 J. N. Shu, W. Wang and H. Cui, *Chem. Commun.* 2015, **51**, 11366-11369.

15 H. L. Zhang, Z. L. Han, X. Wang, F. Li, H. Cui, D. Yang and Z. P. Bian, *ACS Appl. Mater. Interfaces* 2015, **7**, 7599-7604.

16 S. B. Xie, Y. W. Dong, Y. L. Yuan, Y. Q. Chai and R. Yuan, *Anal. Chem.* 2016, **88**, 5218-5224.

17 H. L. Li, M. Eddaoudi, M. O'Keeffe and O. M.Yaghi, *Nature* 1999, **402**, 276-279.

18 W. Y. Gao, Y. Chen, Y. H. Niu, K. Williams, L. Cash, P. J. Perez, L. Wojtas, J. F. Cai, Y. S. Chen and S. Q.Ma, *Angew. Chem. Int. Ed.* 2014, **53**, 2615-2619.

19 Y. Yang, J. J. Liu, C. Liang, L. Z. Feng, T. T. Fu, Z. L. Dong, Y. Chao, Y. G. Li, G. Lu, M. W. Chen and Z. Liu, *ACS nano* 2016, **10**, 2774-2781.

20 L. Wang, Y. Z. Han, X. Feng, J. W. Zhou, P. F. Qi and B. Wang, *Coordin. Chem. Rev.* 2016, **307**, 361-381.

21 Y. R. Miao, Z. Su and K. S. Suslick, *J. Am. Chem. Soc.* 2017, **139**, 4667-4670.

22 J. Y. Lee, O. K. Farha, J. Roberts, K. A. Scheidt, S. T. Nguyen and J. T. Hupp, *Chem. Soc. Rev.* 2009, **38**, 1450-1459.

23 C. D. Wu and M. Zhao, *Adv. Mater.* 2017, **29**, 1605446.

24 C. S. Liu, Z. H. Zhang, M. Chen, H. Zhao, F. H. Duan, D. M. Chen, M. H. Wang, S. Zhang and M. Du, *Chem. Commun.* 2017, **53**, 3941-3944.

25 T. Z. Liu, R. Hu, X. Zhang, K. L. Zhang, Y. Liu, X. B. Zhang, R. Y. Bai, D. L. Li and Y. H. Yang, *Anal. Chem.* 2016, **88**, 12516-12523.

26 Y. J. Cui, Y. F. Yue, G. D. Qian and B. L. Chen, *Chem. Rev.* 2012, **112**, 1126-1162.

27 Z. C. Hu, B. J. Deibert and J. Li, *Chem. Soc. Rev.* 2014, **43**, 5815-5840.

28 X. M. Lin, F. Q. Luo, L. Y. Zheng, G. M. Gao and Y. W. Chi, *Anal. Chem.* 2015, **87**, 4864-4870.

29 K. M. L. Taylor-Pashow, J. Della Rocca, Z. G. Xie, S. Tran and W. B. Lin, *J. Am. Chem. Soc.* 2009, **131**, 14261.

30 X. M. Lin, F. Q. Luo, L. Y. Zheng, Y. W. Chi and G. N. Chen, *Anal. Chem.* 2014, **86**, 1223-1228.

31 C. Y. Xiong, H. J. Wang, W. B. Liang, Y. L. Yuan, R. Yuan and Y. Q. Chai, *Chem. Eur. J.* 2015, **21**, 9825-9832.

32 B. Wu, X. C. Lin, L. Ge, L. Wu and T. W. Xu, *Chem. Commun.* 2013, **49**, 143-145.

33 J. Z. Guo, H. Cui, S. L. Xu and Y. P. Dong, *J. Phys. Chem. C,* 2007, **111**, 606-611.